Atmospheric
Chemistry
and Physics
Discussions

Reversible and irreversible gas-particle partitioning of dicarbonyl compounds observed in the real atmosphere

Jingcheng Hu[1], Zhongming Chen[1], Xuan Qin[1], and Ping Dong[1]

[1]State Key Laboratory of Environmental Simulation and Pollution Control, College of Environmental Sciences and
5   Engineering, Peking University, Beijing, 100871, China

Correspondence to: Zhongming Chen (zmchen@pku.edu.cn)

Abstract. Glyoxal and methylglyoxal are vital carbonyl compounds in the atmosphere and play substantial roles in radical
cycling and ozone formation. The partitioning process of glyoxal and methylglyoxal between the gas and particle phase via
reversible and irreversible pathways could efficiently contribute to secondary organic aerosol (SOA) formation. However, the
10   relative importance of two partitioning pathways still remain elusive, especially in the real atmosphere. In this study, we
launched five field observations in different seasons and simultaneously measured glyoxal and methylglyoxal in the gas and
particle phase. The field-measured gas-particle partitioning coefficients were 5–7 magnitudes higher than the theoretical ones,
indicating the significant roles of reversible and irreversible pathways in the partitioning process. The particulate concentration
of dicarbonyls and product distribution via the two pathways were further investigated using a box model coupled with the
15   corresponding kinetic mechanisms. We recommended the irreversible reactive uptake coefficient γ for glyoxal and
methylglyoxal in different seasons in the real atmosphere, and the average value of 8.0×10^{-3} for glyoxal and 2.0×10^{-3} for
methylglyoxal best represented the the loss of gaseous dicarbonyls by irreversible gas-particle partitioning processes.
Compared to the reversible pathways, the irreversible pathways played a dominant role, with a proportion of more than 90%
in the gas-particle partitioning process in the real atmosphere and the proportion was significantly influenced by relative
20   humidity and inorganic components in aerosols. However, the reversible pathways were also substantial, especially in winter,
with a proportion of more than 10%. These two pathways of dicarbonyls jointly contributed to more than 25% of SOAs in the
real atmosphere. To our knowledge, this study was the first to systemically examine both reversible and irreversible pathways
in the ambient atmosphere, strove to narrow the gap between model simulations and field-measured gas-particle partitioning
coefficients, and revealed the importance of gas-particle processes for dicarbonyls in SOA formation.

25   ## 1 Introduction

Glyoxal and methylglyoxal, the simplest α-dicarbonyls, are recognized as being of great importance in atmospheric chemistry
due to their unique physicochemical properties. The α-dicarbonyl functionality increases their water solubility and reactivity
more than expected. The traditional opinion is that methylglyoxal is less reactive compared to glyoxal due to its unreactive

methyl substitution, while a very recent study noted that methylglyoxal could be more reactive under an atmospheric-relevant

30   concentration (Li et al., 2021). Overall, both of them play crucial roles in radiation balance, air quality, brown carbon formation,

and SOA formation (Laskin et al., 2015; Qiu et al., 2020). Moreover, as major carcinogenic and genotoxic compounds,

dicarbonyls can cause serious damage to human health. They have relatively limited primary sources, except for biomass

burning and biofuel combustion (Zarzana et al., 2018; Zarzana et al., 2017), compared to secondary formation that occurs with

photooxidation of both biogenic volatile organic compounds (VOCs), such as isoprene, and anthropogenic VOCs, such as

35   aromatic hydrocarbons (Lv et al., 2019). Considering the atmospheric sink, glyoxal and methylglyoxal can be lost in the gas

phase by photochemical reactions, oxidation by OH radicals, and dry deposition; however, there is still a missing sink for the

two dicarbonyls (Volkamer et al., 2007).

Gas-particle partitioning was recently found to be the most important removal pathway for both glyoxal and methylglyoxal,

especially in regions like Beijing with high particulate matter (PM) pollution that provides sufficient aerosol surface area.

40   Although with relatively high vapor pressure, glyoxal and methylglyoxal can efficiently partition into the particle phase due

to their α-dicarbonyl functionality. Upon physical adsorption to the particle phase, they can undergo various chemical reactions

and subsequently form larger-molecular-weight products retained in the condensed phase. Moreover, chemical reactions can

in turn accelerate the physical adsorption and greatly contribute to the formation and growth of atmospheric particulate matter.

The chemical reactions occurring in the gas-particle partitioning processes can be divided into reversible pathways, including

45   reversible hydration and self-oligomerization, and irreversible pathways, which can be driven by oxidative radicals and other

reactive compounds. These processes can also efficiently explain observed aerosols properties – including relatively high

oxygenation levels, compositions like organic acids and oligomers, and higher light absorption – that cannot be explained by

traditional absorptive models of gas-particle partitioning (Pankow, 1994; Pankow and James, 1994; Odum et al., 1996).

Many laboratory and model studies have made a great effort to investigate the reversible and irreversible pathways of

50   dicarbonyls to further understand their gas-particle partitioning mechanisms and reveal their contribution to SOA formation.

Fu et al. (2008) found that the modeled SOA concentrations were largely increased when accounting for irreversible uptake of

dicarbonyls in the GEOS-Chem model. Considering the surface-controlled reactive uptake of dicarbonyls into the CMAQ

model, the aerosol uptake of dicarbonyls accounted for more than 45% of total SOA in the eastern US (Ying et al., 2015);

similarly, the contribution of glyoxal and methylglyoxal to SOA formation in China was 14% to 25% and 23% to 28%,

55   respectively (Hu et al., 2017). Although reversible and irreversible pathways of dicarbonyls have been separately investigated

in previous studies, solely incorporating just one pathway into models could lead to a large discrepancy between model results

and observational data, highlighting the importance of comprehensively considering both reversible and irreversible pathways

when quantifying the gas-particle partitioning process of dicarbonyls (Li et al., 2014; Hu et al., 2017; Ling et al., 2020).

Despite increasing interest in dicarbonyls and their gas-particle partitioning processes, the detailed chemical mechanisms of

60 two partitioning pathways remain poorly understood. First, previous studies have exposed seed particles to high concentration

levels of dicarbonyl vapors, from hundred ppb to ppm levels, or used bulk samples; thus, their applicability to the real

atmosphere requires further validation. Second, prior studies always used one constant coefficient to present all heterogeneous

processes occurring on the aerosol, which neglects the influencing factors in real atmospheric partitioning processes. Further

studies have shown that the two pathways in the gas-particle partitioning process for glyoxal and methylglyoxal are rather

65 complex, and their relative contribution to the partitioning process can be influenced by many factors such as relative humidity

(Curry et al., 2018; Shen et al., 2018), particle acidity (Liggio et al., 2005b; Shi et al., 2020), and particle organic/inorganic

components (Kampf et al., 2013). However, there persist controversies in the specific partitioning mechanisms of glyoxal and

methylglyoxal, especially conflicting views on their role in SOA formation, which urgently warrants further investigation.

In this study, five field observations were launched over urban Beijing in four seasons, and glyoxal and methylglyoxal in the

70 gas and particle phase were simultaneously measured. Beijing, as the political center of China, is the most prosperous city with

numerous key environmental issues. Chen et al. (2021) found that the average concentration of dicarbonyls in Beijing is lowest

among key regions with relatively higher $PM_{2.5}$ concentrations, indicating there is a more efficient partitioning process of

dicarbonyls. Thus, it is more environmentally significant to discuss the gas-particle partitioning processes in urban Beijing.

These processes are divided into two pathways: reversible and irreversible. On the basis of field-measured data, we could

75 estimate the product distribution, main influencing factors, and relative importance of the two gas-particle partitioning

pathways for glyoxal and methylglyoxal in the real atmosphere.

2 MATERIALS AND METHOD

2.1 Field sampling and analysis

We performed field observations on the roof of a six-story teaching building (26 m above the ground) on the Peking University

80 campus (39.992°N, 116.304°E) in northwest urban Beijing. The field observations in this study were launched during four

different seasons from 2019 to 2021.

Gaseous carbonyls were collected by adsorption reactions in a 2,4-dinitrophenyl hydrazine (DNPH) cartridge (Sep-Pak; Waters

Corporation). The air samples were first passed through an ozone scrubber (Sep-Pak; Waters Corporation) to eliminate

interference by ozone and then trapped in the DNPH cartridge. To prevent deliquescence of the potassium iodide in the ozone

85 scrubber, the air samples were mixed with ultrapure nitrogen before pumped into the sampling tubing.

Particulate carbonyls were collected by a four-channel ambient particles sampler (TH-16A, Wuhan Tianhong) with Teflon

filters and quartz filters (47 mm, Whatman). The Teflon filters were used to measure the mass concentration of collected $PM_{2.5}$

and the quartz filters were used for carbonyl analysis. Detailed information about field sampling and analysis were provided

in our previous studies (Rao et al., 2016; Qian et al., 2019).

90　　The meteorological station was co-located at our sampling site and provided meteorological parameters. Commom trace gases like NO/NO$_2$, SO$_2$, CO, and O$_3$ were detected online by Thermo 42i, 43i, 48i, and 49i analyzers, respectively. A TEOM 1400A analyzer was applied to measure the mass concentrations of PM$_{2.5}$ and PM$_{10}$, the results of which were consistent with the PM$_{2.5}$ weighing results (Fig. S1). The time solution for all of the above data was 1 min. Detailed information about these five observations is shown in Table S1.

95　　**2.2 Sample extraction and analysis**

The gaseous carbonyl samples were eluted with acetonitrile (HPLC/GC-MS grade), and the particulate carbonyl samples on quartz filter were eluted with acidic DNPH solutions in the flask and then were shaken for 3 h at 4 °C with a rotation rate of 180 rpm in an oscillator (Shanghai Zhicheng ZWY 103D). The derived solutions were placed in darkness for 12-24 h to ensure complete derivatization, and then they were analyzed by high-performance liquid chromatography-ultraviolet (HPLC-UV) for

100　　separation and detection. The limit of detection (LOD) of this method was 50 pptv for gaseous carbonyls and 1 ng·m^{-3} for particulate carbonyls. They were calibrated using a mixing standard solution with a concentration range of 0.1–10 μM, and the linearity was indicated by a correlation of determination (r^2) of at least 0.999. The detailed analysis method was presented in our previous study (Wang et al., 2009).

The Teflon samples were also extracted by deionized water using an ultrasonic bath for 30 min at room temperature. The

105　　extracted solutions were analyzed by ion chromatography (Integrion and Dionex ICS 2000, USA) to measure the water-soluble inorganic compounds (Na$^+$, NH$_4^+$, K$^+$, Mg^{2+}, Ca^{2+}, Cl$^-$, NO$_3^-$, and SO$_4^{2-}$) and low-molecular-weight organic acids (formate, acetate, and oxalate) in aerosols.

2.3 Estimation of effective partitioning coefficient

To estimate the effective partitioning process of gas-phase carbonyls to the particle phase, we could use Pankow's absorptive

110　　partitioning theory for the gas-organic phase (Eqs. (1), (2)) (Odum et al., 1996) and Henry's law for the gas-liquid phase (Eq. (3)):

$$K_p^f = \frac{C_p}{C_g \times TSP} \tag{1}$$

$$K_p^t = \frac{RTf_{om}}{10^6 MW_{OM} \zeta p_L^0} \tag{2}$$

$$K_H^f = 10^3 \frac{c_p}{c_g \times M \times ALWC/\rho_{water}} \tag{3}$$

115　　In Eq. (1), K_p^f (m^3·μg^{-1}) is the field-measured gas-particle partitioning coefficient; C_p (μg·m^{-3}) and C_g (μg·m^{-3}) are the concentrations of dicarbonyls in the particle and gas phase, respectively; and TSP (μg·m^{-3}) is the mass concentration of

suspended particles (mass concentrations of PM$_{2.5}$ were used in this study). In Eq. (2), K_p^t (m^3·µg^{-1}) are the theoretical gas-particle partitioning coefficients determined by Pankow's absorptive model, f_{om} is the absorbing fraction of total particulate mass, MW$_{OM}$ (g·mol^{-1}) is the mean molecular weight of the organic phase, and ζ is the activity coefficient of target compounds.

In the estimation of K_p^t in this study, f_{om} and ζ are unity and MW$_{OM}$ = 200 g·mol^{-1}, as used in previous studies (Healy et al., 2008; Williams et al., 2010; Xie et al., 2014; Shen et al., 2018), and p_L^0 (Pa) is the supercooled vapor pressure of compounds as a pure liquid at temperature T, which is calculated by the extended aerosol inorganic model (E-AIM, http://www.aim.env.uea.ac.uk/aim/ddbst/pcalc_main.php) (Clegg et al., 1998). In Eq. (3), K_H^f (M·atm^{-1}) is the field-derived effective Henry's law coefficient; c_P (µg·m^{-3}) and c_g (atm) are particle- and gas-phase concentrations of carbonyls, respectively; ALWC (µg·m^{-3}) is the aerosol liquid water content calculated by the thermodynamic model ISORROPIA-II (forward model, metastable state), the results of which are comparable to the actual measured contents confirmed by previous studies (Guo et al., 2015)..

3 RESULT AND DISCUSSION

3.1 Observation results and partitioning coefficients calculation

3.1.1 Dicarbonyls in the gas and particle phase

We launched five field observations in different seasons. Table S1 details the information about the field observations, including observation periods, sample volume, and meteorological parameters. We totally collected 387 gas-phase samples and 130 particle-phase samples in four seasons. In these samples, carbonyls were simultaneously measured in both gas phase and particle phase. Ten carbonyls were measured in the gas phase and six carbonyls were measured in the particle phase. In this study, we mainly discuss the gas-particle partitioning processes of glyoxal and methylglyoxal because of their significant roles in atmospheric chemistry.

Figure 1 and Table 1 show the temporal characteristics and seasonal variation of glyoxal and methylglyoxal, respectively. Gaseous dicarbonyls showed obvious seasonal variation. Concentrations in summer (0.99 ± 0.59 ppbv) were generally much higher than in other seasons, followed by autumn and spring, and the concentrations in winter were the lowest. This seasonal variation could be partly attributed to the higher temperature and more intensive radiation in summer, which could greatly enhance the secondary formation of gaseous carbonyls via photochemical reactions. The diurnal variation in the dicarbonyls during summer support this interpretation of the data; gas-phase dicarbonyls exhibited obviously diurnal variations in summer, whereas this variation was irregular in other seasons (Fig. S2). The concentration levels of gaseous dicarbonyl in summer rapidly increased after sunrise, remained relatively high during the daytime (12:00–14:00), and then decreased at dusk. Although methylglyoxal has a shorter lifetime compare to glyoxal (GL 2.9 h vs. MG 1.6 h) (Fu et al., 2008), its gas-phase

concentration levels were generally higher than those of glyoxal, consistent with previous studies (Rao et al., 2016; Mitsuishi et al., 2018; Qian et al., 2019), mainly due to the relatively larger production from isoprene and acetone for methylglyoxal. The concentrations of particulate dicarbonyls were an order of magnitude smaller than the gaseous concentrations using the unit of nanogram per cubic meter of air (ng/m^3 air). The average particulate glyoxal and methylglyoxal were 19.37 and 11.24

150   ng/m^3, respectively, which were slightly higher than previously reported values (Zhu et al., 2018; Shen et al., 2018; Cui et al., 2021; Qian et al., 2019). Dicarbonyls measured in the particle phase also showed obvious seasonal variation. The particulate concentrations of the two dicarbonyls in winter (43.38 ± 32.42 ng/m^3 air) were 2–2.3 times higher than those in other seasons, suggesting that the dicarbonyls were more favored into the particle phase in winter. Moreover, particulate dicarbonyls in different seasons exhibited the same diurnal variation (Fig. S2). The particulate concentrations of dicarbonyls in daytime were

155   generally higher than those in nighttime, especially in winter.

3.1.2 Gas-particle partitioning coefficient

Dicarbonyls could partition between gas and aerosol phases or the liquid phase, following Pankow's absorptive partitioning theory or Henry's law, respectively, as listed in Table 2. Both gas-particle partitioning coefficient (K_p^f) and effective Henry's law coefficient (K_H^f) were calculated on the basis of field-measured data and were in the range of 10^{-4}–10^{-2} m$^3 \cdot \mu$g^{-1} and 10^6–

160   10^8 M·atm^{-1}, respectively. The partitioning coefficient values of the two dicarbonyls exhibited the same seasonal variation, as winter and spring > autumn > summer. A higher aerosol concentration accompanied by higher aerosol surface area concentration and lower relative humidity resulted in a higher partitioning coefficient in winter and spring, when heavy pollution and sandstorms always occurred. In the case of temperature variation varied from 265.53 K to 310.75 K in different seasons, lower temperature promoted the partitioning processes as K_p^f values for the dicarbonyls and temperature showed

165   negative correlation with significant difference (p < 0.001) (Fig. S3). Moreover, The K_p^f and K_H^f values of glyoxal were always higher than those of methylglyoxal, implying the former was more likely to partition to the particle phase; this could be attributed to their different structures. Glyoxal were more soluable and reactive because of the adjacent electron-poor aldehydic carbons, whereas methylglyoxal was more stable due to the reduced electron-deficient ketone moiety (Kroll et al., 2005).

170   Both K_p^f and K_H^f were relatively closed to those found in previous field-measured studies (Shen et al., 2018; Qian et al., 2019; Cui et al., 2021). However, compared with the theoretical partitioning coefficients K_p^t calculated by Pankow's absorptive theory, K_p^f values were approximately 5–7 orders of magnitudes higher than the corresponding K_p^t values. The influencing factors in Pankow's absorptive model, like the activity coefficient ζ or absorbing fraction f_{om}, could not explain this great difference between the field-measured values and the theoretical ones. The underestimation of gas-particle

175   partitioning coefficients can be attributed to the misidentification of condensed phase species produced in heterogeneous

chemical reactions. Similarly, K_H^f values were approximately 2–5 orders of magnitudes higher than the theoretical Henry's law coefficient K_H^t calculated in pure water. The discrepancy could be explained by the complex components in aerosol liquid water. Figure S4 presents the Setschenow plot of dicarbonyls versus aqueous sulfate, nitrate, and ammonia (SNA) concentration in aerosol. The negative salting constant indicated the "salting in" effects, which could result in exponential

180   solubility, for both glyoxal and methylglyoxal in the real atmospheric. Moreover, both K_p^f and K_H^f of dicarbonyls were more than one magnitude higher than the reported laboratory partitioning coefficient values from chamber experiments (Healy et al., 2008; Healy et al., 2009), indicating that the real atmosphere is more favorable for the partitioning of gaseous dicarbonyls to the particle phase. Actual atmospheric environment conditions and complex particle compositions, such as higher ionic strength, could greatly affect the partitioning process and the chemical reactions in the aerosols.

185   To narrow the large discrepancy between field-measured partitioning coefficients and theoretical (or laboratory) ones, we needed to further investigate the mechanism and product distribution of chemical reactions occurring in the aerosols during the partitioning processes. The products of the reversible pathway mostly have lower saturated vapor pressure, and thus leading to higher partitioning coefficients compared to monomer dicarbonyls. For example, the calculated vapor pressures of the products of glyoxal hydration and dimerization are, respectively, 5 and 10 orders of magnitudes less than that of glyoxal

190   monomer (Hastings et al., 2005). Moreover, the products of the irreversible pathway, such as organic acids produced in radical chemistry, also have lower vapor pressure and efficiently contribute to the underestimation of partitioning coefficients. The following sections further discuss the mechanism and product distribution of reversible and irreversible pathways to explain the partitioning process of dicarbonyls.

3.2 Reversible pathways

195   Gas-particle partitioning of dicarbonyls via a reversible pathway mainly consists of hydration and self-oligomerization. Since glyoxal and methylglyoxal had high water solubility and reactivity, they could easily dissolve into aerosol liquid water and form hydrates, which are more reactive than their counterparts and could participate in continuous reactions to form higher-molecular-weight oligomers. Hemiacetal/acetal formation (Loeffler et al., 2006) and aldol condensation (Haan et al., 2009) are the most thermodynamically favored oligomer reactions for glyoxal and methylglyoxal, respectively. The proposed

200   mechanism for the reversible formation of glyoxal and methylglyoxal in aerosols is shown in Fig. S5. Overall, since the products of the reversible pathway, including hydrates and oligomers, are thermodynamically unstable and could easily revert to their original monomer form during extraction and analysis, their total concentration could be presented as the measured particle-phase dicarbonyls from sampled quartz filters. Since glyoxal and methylglyoxal have similar trend under different conditions, we focused on the total concentration of the two dicarbonyls in the following discussion. As shown in Fig. 2a, the

205   particulate concentration of dicarbonyls via a reversible pathway is strongly dependent on RH. It increased significantly when

RH increased from <10% to 60%; however, from 60% to 80% RH, it exhibited the opposite trend and decreased with increasing RH. Moreover, under high RH conditions, the particulate concentration of dicarbonyls via a reversible pathway had a strong and positive dependence on particle acidity (pH). The product distribution of the reversible formation could well explain this phenomenon.

210   To roughly estimate the product distribution of the reversible pathway in the real atmosphere, we simplified reaction mechanisms and calculated the product distribution on the basis of the equilibrium constant reported in previous literature (Table S2). Generally, more dicarbonyls existed in oligomer forms (83.5% for glyoxal and 80.8% for methylglyoxal) than in hydrate forms (16.3% for glyoxal and 20.8% for methylglyoxal) in the reversible formation. Moreover, their distribution exhibited obvious seasonal variations. Summer had the highest proportion of hydrate forms (52.80% for GL and 35.10% for

215   MG), while winter had the highest proportion of oligomer forms (86.15% for GL and 86.31% for MG). Detailed information is shown in Table S3. The seasonal variation could be attributed to the RH in different seasons – relatively high in summer and low in winter. As shown in Fig. 2b, the product distribution of the reversible formation has a strong dependence on RH. The proportion of dicarbonyls in hydrate forms increased with increasing RH and could reach more than 75% in high RH, while the proportion of dicarbonyls in oligomer forms exhibited the opposite trend. Hydrates play a dominant role in dilute solutions

220   under high RH conditions with a relatively high aerosol liquid water concentration, which might hinder oligomer formation. And large quantities of oligomers, including dimers and trimers, would form until the aerosol liquid concentration became greater than 1 M (Liggio et al., 2005b) when RH decreased.

Combined with the vapor pressure of dominant products, their gas-particle partitioning coefficient can be roughly estimated and can effectively fit the field-measured values, as shown in Fig. 2c. The estimated gas-particle partitioning coefficients in

225   this study are five orders of magnitude higher than the theoretical ones but still 1–2 orders of magnitude lower than the field-measured coefficients, especially in winter. The difference between the estimated partitioning coefficients and the field-measured ones suggests that the current understanding of the equilibrium in reversible formations cannot reasonably explain the gas-particle partitioning processes of dicarbonyls. There still exist extra pathways of reversible formation. Cross-oligomerization of glyoxal and methylglyoxal is nonnegligible and could form similar molecular structure products and

230   contribute to SOA yield (Schwier et al., 2010). Esterification and amination of diols also occur in aerosol liquid water but are negligible compared to hydration and polymerization (Zhao et al., 2006). However, these reactions are not further discussed here. The hydrates and oligomers mentioned above are the dominant forms of glyoxal/methylglyoxal in the particle phase, while the higher molecular oligomers up to nonamer could also exist with a relatively smaller but still significant fraction at equilibrium. Although the reactions are thermodynamically reversible, upon evaporation of the aerosol liquid water, the

235   oligomer formation is faster than the evaporation of dehydrated dicarbonyls, and the dicarbonyl evaporation is limited (Liggio et al., 2005b; Loeffler et al., 2006). This results in relatively stable oligomers and yielding SOA. Moreover, other nucleophilic

species may also form oligomers with glyoxal and methylglyoxal and effectively prevent their evaporation. Besides reversible pathways, higher carbon number products with lower volatility were mainly formed through irreversible pathways, like radical reactions (e.g., OH radicals), which are fully discussed in the next section.

3.3 Irreversible pathways

3.3.1 Irreversible pathways driven by hydroxyl radicals

Reactive uptake driven by hydroxyl radicals (OH) is the dominant process for glyoxal and methylglyoxal in their irreversible gas-particle partitioning pathways. Compared to other irreversible pathways, like imidazole formation, glyoxal/methylglyoxal + OH chemistry occurs on much shorter timescales (Teich et al., 2016). The reaction is the initial step for most radical-based chemistry of glyoxal/methylglyoxal and has been proven to be an important source of SOA in both cloud/fog droplets and wet aerosols (Tan et al., 2012; Lim et al., 2013), producing low-volatility products such as organic acids, large multifunctional humic-like substances, and oligomers. The proposed mechanism for the irreversible pathway of glyoxal and methylglyoxal driven by hydroxyl radicals in aerosols is shown in Fig. S6. The OH radicals in aerosol liquid water are mainly from the direct uptake of gas-phase OH radicals with a Henry's law constant of 30 M/atm (Faust and Allen, 1993) and Fenton reactions, and Fenton reactions are closely related to hydrogen peroxide, iron ions, and manganese ions in the particle phase. The sources of OH radicals are one of the major uncertainties in SOA formation (Ervens et al., 2014).

The irreversible reactive uptake coefficient γ could efficiently describe the irreversible pathway of the gas-particle partitioning process of dicarbonyls driven by OH radicals. We could estimate the reactive uptake coefficients γ based on the effective Henry's constant via theory calculation (Hanson et al., 1994; Curry et al., 2018) and then calculate the effective uptake rate $k_{eff, uptake}$, following Eqs. (4)–(7):

$$\frac{1}{\gamma} = \frac{1}{\alpha} + \frac{v}{4RTH^*\sqrt{k^l D_{aq}}} \times \frac{1}{[cothq-1/q]} \tag{4}$$

$$v = \sqrt{\frac{8RT}{\pi M_X}} \tag{5}$$

$$q = R_p/l = R_p/\sqrt{\frac{D_{aq}}{k^l}} \tag{6}$$

$$k_{eff, uptake} = \frac{1}{4} v \times \gamma \times A_{surf} \tag{7}$$

where γ is the dimensionless uptake coefficient, v (m·s^{-1}) is the gas-phase thermal velocity of glyoxal/methylglyoxal, D_{aq} (m^2·s^{-1}) is the diffusion coefficient in the liquid phase, α is the dimensionless mass accommodation coefficient, H* (M·atm^{-1}) is the effective Henry's law constant calculated by field-measured data in Table 2, R is the universal gas constant, k^l (s^{-1}) is the first-order aqueous loss rate, M_X (kg·mol^{-1}) is the average molar mass of gas-phase dicarbonyls, q is the parameter for measuring in-particle diffusion limitations, R_p (m) is the particle radius, l (m) is the diffusion reactive length, $k_{eff, uptake}$ (s^{-1}) is

265   the effective uptake rate, and A_{surf} ($m^2 \cdot m^{-3}$) is the aerosol surface area density. This formulation is based on the effective Henry's law constant under high RH conditions (RH > 40%). Moreover, the formulation describes the reactive uptake due to irreversible multiple-phase loss processes in the presence of OH. The uncertainty in the γ calculation is mainly attributed to the uncertainty in OH concentration, which was 3×10^{-12} M on average and varied from 5.5×10^{-14} to 8×10^{-12} M (Herrmann et al., 2010).

The calculated γ and $k_{eff, uptake}$ values for different seasons are listed in Table 3. The reactive uptake coefficients of glyoxal were

270   in the range 10^{-4}–10^{-2}, and the average value of 8.0×10^{-3} in this study was closed to the ones representing the loss of glyoxal by surface uptake during the KORUS-AQ campaign in a very recent studies (Kim et al., 2022). And the value slightly exceeded the one commonly used in model simulations ($\gamma = 2.9\times10^{-3}$), which was based on an experimental study for $(NH_4)_2SO_4$ aerosols at 55% RH (Liggio et al., 2005a), and also far outweighs the uptake coefficients of glyoxal on clean and acidic gas-aged mineral particles ($\gamma = 10^{-6}$–10^{-4}) (Shen et al., 2016), implying that a real atmospheric aerosol provides a far more reactive

275   interface for physiochemical processes than that of mineral particles. Moreover, the reactive uptake coefficients of methylglyoxal were slightly lower than those for glyoxal, with an average value of 2.0×10^{-3}. Conflicting with previous experimental results, methylglyoxal exhibited unexpected salting-in effects in real atmospheric particles and had much higher uptake coefficients, which could be attributed to the increased reactivity of methylglyoxal with a high uptake coefficient under an atmospheric relevant concentration (Li et al., 2021). The γ values for both glyoxal and methylglyoxal exhibited similar

280   seasonal variations, which were lowest in summer and reached their highest in winter. This seasonal variation could be attributed to RH variation and particle composition. Moreover, the effective uptake rate ($k_{eff, uptake}$), which is regarded as a pseudo-first-order reaction rate, is a net result of competition between reversible and irreversible processes, and it varied from 10^{-4} s^{-1} to 10^{-5} s^{-1} in the real atmosphere in this study. As shown in Fig. 3a, the negative dependence of $k_{eff, uptake}$ on RH also confirmed that the irreversible uptake of dicarbonyls could be inhibited in high RH conditions. And the relatively low SNA

285   concentration under high RH conditions also attenuated the irreversible uptake as the weakening of ion effects (Figure 3b). Whereas, for a given RH, uptake coefficients γ for both glyoxal and methylglyoxal showed a weak dependence on the ratio of SNA (S:A and S:N) with significant scatter (Fig. S7).

Moreover, it was worth noting that under extremely low RH (<40%), the aerosol was not completely deliquescent, and the uptake coefficients based on Henry's law could not explain the irreversible pathways. Previous research indicated that the

290   irreversible uptake of dicarbonyls could still occur under a low RH condition (Liggio et al., 2005a; De Haan et al., 2018), and that these uptake values were generally lower due to the inefficient reactive uptake process onto the crystallized aerosols.

3.3.2 Reactive uptake of dicarbonyl compounds

We could not directly measure the particulate concentration of dicarbonyls via an irreversible pathway, as the dicarbonyls irreversibly reacted with oxidative radicals on aerosols. To quantitively evaluate the contribution of the irreversible pathway

Atmospheric
Chemistry
and Physics
Discussions

295 of dicarbonyls, we calculated their average concentration based on Eqs. (S1)–(S5) in the Supplement with the calculated γ

values in this study. The samples estimated here were collected under high RH conditions (RH > 40%) because of the

calculation limitation of irreversible uptake coefficients.

The total particulate concentration of glyoxal and methylglyoxal via irreversible pathway varied from several to more than

100 nanograms per microgram PM$_{2.5}$ (ng/μg PM$_{2.5}$), and it was strongly dependent on RH, as shown in Fig. 3c. Since the

300 irreversible uptake coefficients γ of dicarbonyls tended to decrease with increasing RH due to the "salting-in" effects, both

glyoxal and methylglyoxal in this study exhibited high solubility in low RH conditions, where the aerosol water was coupled

with concentrated inorganic solutions and relatively high ionic strength. Moreover, the total particulate concentrations of

dicarbonyls were positively dependent on particle acidity under high RH conditions, while there were no obvious correlations

under low RH conditions.

305 To further discuss the product distribution of the reaction of glyoxal/methylglyoxal with hydroxyl radicals, we used the kinetic

mechanisms of glyoxal/methylglyoxal + OH chemistry proposed by Lim et al. (2013) on the basis of a 0-D box model with a

steady-state approach. The average OH radical concentration setting in the modeling was 3.2×10^{-12} M, which is based on the

hypothesis of the Henry equilibrium of OH radicals between the gas and particle phase (Sander, 2015; Shen et al., 2018).

Oxalate can be considered as a tracer for this aqueous chemistry, since it does not have any other significant chemical sources.

310 Oxalate was detected in the particle-phase samples by ion chromatography. The modeling results of oxalate concentration

agreed well with the measured values, and their deviations were in the considered range (Fig. S7). Meanwhile, we can estimate

the distribution of major products in irreversible glyoxal/methylglyoxal-OH radical chemistry under different RH conditions,

as illustrated in Figure 3d. Generally, oxalate is the major product in wet aerosols, contributing ~60%, and its proportion

increases with increasing RH. Besides oxalate, oligomers also play significant roles in glyoxal/methylglyoxal-OH radical

315 chemistry with a contribution of ~30%, and their proportion is maximum under relatively low RH conditions. The RH

dependence of the product distribution could mainly be attributed to the particulate concentration of glyoxal/methylglyoxal,

which significantly affects the OH radical chemistry. With relatively high carbonyl concentrations (0.1–10 M) in aerosol liquid

water, self-reactions of organic molecules become more favorable, resulting in new carbon–carbon bonds and high molecular

weight oligomers via radical–radical chemistry (Lim et al., 2013). Moreover, besides OH radical chemistry, reaction with

320 sulfate and ammonium also contribute to the oligomer formation and irreversible uptake of gaseous dicarbonyls (Ortiz-

Montalvo et al., 2014; Lim et al., 2016; Lin et al., 2015). The oligomer proportion could be more than 30% in concentrated

carbonyl solutions (~0.1 M) and only account for 1% in diluted solutions (~0.01 M).

3.4 Relative importance of two partitioning pathways

Table 4 summarizes the particulate concentration of glyoxal and methylglyoxal via reversible and irreversible pathways in

325 different seasons. The average particulate concentrations of glyoxal (0.43 ng/μg in the reversible pathway and 24.26 ng/μg in the irreversible pathway) were generally higher than those of methylglyoxal (0.25 ng/μg in the reversible pathway and 16.53 ng/μg in the irreversible pathway), mainly due to the relatively higher water solubility and reactivity of glyoxal. Comparing two gas-particle partitioning processes, the irreversible pathway played extremely dominant roles and generally accounted for 96.7% and 95.0% for glyoxal and methylglyoxal, respectively. The proportion of the irreversible pathway varied from 90% to

330 99.9% and reached its highest in summer for glyoxal (98.8%) and in autumn for methylglyoxal (99.2%), while it was minimum in winter (92.9% for glyoxal and 92.8% for methylglyoxal). Overall, the irreversible pathway played a dominant role in the gas-particle partitioning process for both glyoxal and methylglyoxal in the real atmosphere, while the reversible pathway was also substantial and nonnegligible, especially in winter, with an proportion of ~10%. Furthermore, as discussed above, the particulate concentrations of dicarbonyls and their relative importance were influenced by environmental factors such as

335 relative humidity and particle composition, which could jointly influence both the reversible and irreversible pathways of dicarbonyls. As shown in Figure 4, the proportion of irreversible pathways in the gas-particle partitioning process for dicarbonyls increased with aqueous SNA concentrations, and reached maxium when SNA concentrations were more than 100 M under low RH conditions.

Comprehensively considering the contribution of two pathways in partitioning processes could be conductive to ambient

340 dicarbonyls simulations. Ling et al. (2020) found that the observation and simulation of the gas-phase concentration level of dicarbonyls could reach reasonable agreement when the irreversible uptake and reversible partitioning were incorporated into the model, as these jointly contribute ~62% to the sink of dicarbonyls. Moreover, the contribution of gas-particle partitioning processes of dicarbonyls to SOA formation were higher as the two partitioning pathways were jointly considered. In this study, gas-particle partitioning processes of dicarbonyls accounted for a relatively large proportion of total particle mass (PM$_{2.5}$), on

345 the average of ~5% considering both reversible and irreversible gas-particle partitioning pathways. Since a large fraction of PM$_{2.5}$ mass in Beijing consists of SOAs (~30%) (Huang et al., 2014), we could roughly estimate the contribution of gas-particle partitioning processes of dicarbonyls to SOA yields (by mass). There were approximately 25% SOAs formed from glyoxal and methylglyoxal in this study. However, the particulate dicarbonyls calculated here only contained simple reversible pathways and irreversible pathways driven by OH radicals. More complicated chemical processes like NO$_3$ radical chemistry

350 were not considered, which still resulted in the underestimation of their contribution to SOA formation.

4 Conclusions

We simultaneously measured glyoxal and methylglyoxal concentration in the gas and particle phase in different seasons over urban Beijing. Based on field-measured data, the field-derived gas-particle partitioning coefficients were calculated and found

to be 5–7 magnitudes higher than the theoretical values. Such a large discrepancy provides field evidence that the gas-particle

355 partitioning process does not occur by physical absorption alone but also results from the combined and simultaneous effects

of reversible and irreversible pathways. Hydration and oligomerization occurred in the reversible pathway, producing

compounds with lower volatility in the condensed phase, and the irreversible pathway could accelerate the uptake of gaseous

dicarbonyls. The two pathways jointly contributed to the underestimation of gas-particle partitioning of dicarbonyls.

This study systemically considers both reversible and irreversible pathways in the ambient atmosphere for the first time.

360 Compared to the reversible pathways, the irreversible pathways play a dominant role in the gas-particle partitioning process

for dicarbonyls, accounting for ~90% of this process. We recommend the irreversible reactive uptake coefficient for glyoxal

and methylglyoxal in different seasons in the real atmosphere. The values we calculated here are higher than those used in

model simulations to date, especially for methylglyoxal which exhibits an unexpected salting-in effect under an atmospheric-

relevant concentration. We expect the application of these parameterizations will increase the calculated contribution of

365 irreversible uptake of dicarbonyls to SOA formation and narrow the gap between model predictions and field measurements

of ambient dicarbonyl concentrations. Moreover, relative humidity and inorganic particle compositions are defined as the most

important factor influencing particulate concentration and product distribution of dicarbonyls via both reversible and

irreversible pathways, implying the significance of considering different RH conditions in dicarbonyl SOA simulations.

Furthermore, we note that there may be other potential explanations for the increase in particulate concentrations and the

370 uncertainty in the gas-particle partitioning process. Physical adsorption of dicarbonyls could be enhanced by water-soluble

organics and mineral dust. Other reversible pathways, like adducts formed from glyoxal with inorganic species, like sulfate

and ammonia, could also promote the gas-particle partitioning process. Irreversible pathways driven by other oxidants, like

NO_3 radicals, can also perform a substantial role. Shen et al. (2016) found that glyoxal could irreversibly produce formic acid,

glycolic acid, and oligomers on particles without illumination or extra oxidants. Besides gas-particle partitioning, particulate

375 dicarbonyls formed via the heterogeneous reaction of VOCs could contribute to the uncertainty in partitioning research. Dong

et al. (2021) recently revealed that aqueous photooxidation of toluene could yield glyoxal and methylglyoxal via a ring-

cleavage process. Overall, the real gas-particle partitioning process of glyoxal and methylglyoxal is more complicated and

their contribution to SOA formation is still indistinct; thus, more laboratory experiments and field measurements are urgently

needed to improve our understanding of the gas-particle partitioning process for glyoxal and methylglyoxal.

380

Author contributions. In the framework of the five field measurements in different seasons, ZC and JH designed the study, and

JH performed all carbonyl measurements used in this study, analyzed the data, and wrote the paper. ZC helped interpret the

Atmospheric
Chemistry
and Physics
Discussions

385 results, guided the writing, and modified the manuscript. XQ and PD contributed to the methods of sampling and analyzing gas- and particle-phase carbonyls. All authors discussed the results and contributed to the final paper.

Competing interests. The authors declare that they have no conflict of interest.

Atmospheric
Chemistry
and Physics
Discussions

Reference

395 Chen, X., Zhang, Y., Zhao, J., Liu, Y., Shen, C., Wu, L., Wang, X., Fan, Q., Zhou, S., and Hang, J.: Regional modeling of secondary organic aerosol formation over eastern China: The impact of uptake coefficients of dicarbonyls and semivolatile process of primary organic aerosol, Science of the Total Environment, 793, 148176, 10.1016/j.scitotenv.2021.148176, 2021.

Clegg, S. L., Brimblecombe, P., and Wexler, A. S.: Thermodynamic Model of the System H+-NH4+-SO42--NO3--H2O at Tropospheric Temperatures, Journal of Physical Chemistry A, 102, 2137-2154, 1998.

400 Cui, J., Sun, M., Wang, L., Guo, J., Xie, G., Zhang, J., and Zhang, R.: Gas-particle partitioning of carbonyls and its influencing factors in the urban atmosphere of Zhengzhou, China, Science of the Total Environment, 751, 142027, 10.1016/j.scitotenv.2020.142027, 2021.

Curry, L. A., Tsui, W. G., and McNeill, V. F.: Technical note: Updated parameterization of the reactive uptake of glyoxal and methylglyoxal by atmospheric aerosols and cloud droplets, Atmospheric Chemistry and Physics, 18, 9823-9830, 10.5194/acp-405 18-9823-2018, 2018.

De Haan, D. O., Jimenez, N. G., de Loera, A., Cazaunau, M., Gratien, A., Pangui, E., and Doussin, J. F.: Methylglyoxal Uptake Coefficients on Aqueous Aerosol Surfaces, Journal of Physical Chemistry A, 122, 4854-4860, 10.1021/acs.jpca.8b00533, 2018.

Dong, P., Chen, Z., Qin, X., and Gong, Y.: Water Significantly Changes the Ring-Cleavage Process During Aqueous Photooxidation of Toluene, Environmental Science & Technology, 55, 16316-16325, 10.1021/acs.est.1c04770, 2021.

410 Ervens, B., Sorooshian, A., Lim, Y. B., and Turpin, B. J.: Key parameters controlling OH-initiated formation of secondary organic aerosol in the aqueous phase (aqSOA), Journal of Geophysical Research: Atmospheres, 119, 3997-4016, 10.1002/2013jd021021, 2014.

Faust, B. C. and Allen, J. M.: Aqueous-phase photochemical formation of hydroxyl radical in authentic cloudwaters and fogwaters, Environmental Science & Technology, 27, 113-122, 1993.

415 Fu, T.-M., Jacob, D. J., Wittrock, F., Burrows, J. P., Vrekoussis, M., and Henze, D. K.: Global budgets of atmospheric glyoxal and methylglyoxal, and implications for formation of secondary organic aerosols, Journal of Geophysical Research, 113, 10.1029/2007jd009505, 2008.

Guo, H., Xu, L., Bougiatioti, A., Cerully, K. M., and Weber, R. J.: Fine-particle water and pH in the southeastern United States, Atmospheric Chemistry and Physics, 15, 5211-5228, 2015.

420 Haan, D. O. D., Corrigan, A. L., Smith, K. W., Stroik, D. R., Turley, J. J., Lee, F. E., Tolbert, M. A., Jimenez, J. L., Cordova, K. E., and Ferrell, G. R.: Secondary organic aerosol-forming reactions of glyoxal with amino acids, Environmental Science & Technology, 43, 2818, 2009.

Hanson, D. R., Ravishankara, A. R., and Solomon, S.: Heterogeneous reactions in sulfuric acid aerosols: A framework for model calculations, Journal of Geophysical Research Atmospheres, 99, 3615-3629, 1994.

425 Hastings, W. P., Koehler, C. A., Bailey, E. L., and Haan, D. O. D.: Secondary organic aerosol formation by glyoxal hydration and oligomer formation: humidity effects and equilibrium shifts during analysis, Environmental Science & Technology, 39, 8728-8735, 2005.

Healy, R. M., Temime, B., Kuprovskyte, K., and Wenger, J. C.: Effect of relative humidity on gas/particle partitioning and aerosol mass yield in the photooxidation of p-xylene, Environmental Science & Technology, 43, 1884-1889, 2009.

430 Healy, R. M., Wenger, J. C., Metzger, A., Duplissy, J., Kalberer, M., and Dommen, J.: Gas/particle partitioning of carbonyls in the photooxidation of isoprene and 1,3,5-trimethylbenzene, Atmospheric Chemistry and Physics, 8, 2008.

Herrmann, H., Hoffmann, D., Schaefer, T., Brauer, P., and Tilgner, A.: Tropospheric aqueous-phase free-radical chemistry: radical sources, spectra, reaction kinetics and prediction tools, Chemphyschem, 11, 3796-3822, 10.1002/cphc.201000533, 2010.

435   Hu, J., Wang, P., Ying, Q., Zhang, H., Chen, J., Ge, X., Li, X., Jiang, J., Wang, S., Zhang, J., Zhao, Y., and Zhang, Y.: Modeling biogenic and anthropogenic secondary organic aerosol in China, Atmospheric Chemistry and Physics, 17, 77-92, 10.5194/acp-17-77-2017, 2017.

Huang, R. J., Zhang, Y., Bozzetti, C., Ho, K. F., Cao, J. J., Han, Y., Daellenbach, K. R., Slowik, J. G., Platt, S. M., Canonaco, F., Zotter, P., Wolf, R., Pieber, S. M., Bruns, E. A., Crippa, M., Ciarelli, G., Piazzalunga, A., Schwikowski, M., Abbaszade, G.,
440   Schnelle-Kreis, J., Zimmermann, R., An, Z., Szidat, S., Baltensperger, U., El Haddad, I., and Prevot, A. S.: High secondary aerosol contribution to particulate pollution during haze events in China, Nature, 514, 218-222, 10.1038/nature13774, 2014.

Kampf, C. J., Waxman, E. M., Slowik, J. G., Dommen, J., Pfaffenberger, L., Praplan, A. P., Prevot, A. S., Baltensperger, U., Hoffmann, T., and Volkamer, R.: Effective Henry's law partitioning and the salting constant of glyoxal in aerosols containing sulfate, Environmental Science & Technology, 47, 4236-4244, 10.1021/es400083d, 2013.

445   Kim, D., Cho, C., Jeong, S., Lee, S., Nault, B. A., Campuzano-Jost, P., Day, D. A., Schroder, J. C., Jimenez, J. L., Volkamer, R., Blake, D. R., Wisthaler, A., Fried, A., DiGangi, J. P., Diskin, G. S., Pusede, S. E., Hall, S. R., Ullmann, K., Huey, L. G., Tanner, D. J., Dibb, J., Knote, C. J., and Min, K.-E.: Field observational constraints on the controllers in glyoxal (CHOCHO) reactive uptake to aerosol, Atmospheric Chemistry & Physics, 22, 805-821, 10.5194/acp-22-805-2022, 2022.

Kroll, J. H., Ng, N. L., Murphy, S. M., Varutbangkul, V., Flagan, R. C., and Seinfeld, J. H.: Chamber studies of secondary
450   organic aerosol growth by reactive uptake of simple carbonyl compounds, Journal of Geophysical Research, 110, 10.1029/2005jd006004, 2005.

Laskin, A., Laskin, J., and Nizkorodov, S. A.: Chemistry of atmospheric brown carbon, Chem Rev, 115, 4335-4382, 10.1021/cr5006167, 2015.

Li, X., Rohrer, F., Brauers, T., Hofzumahaus, A., Lu, K., Shao, M., Zhang, Y. H., and Wahner, A.: Modeling of HCHO and
455   CHOCHO at a semi-rural site in southern China during the PRIDE-PRD2006 campaign, Atmospheric Chemistry and Physics,14,22(2014-11-21), 14, 2014.

Li, Y., Ji, Y., Zhao, J., Wang, Y., Shi, Q., Peng, J., Wang, Y., Wang, C., Zhang, F., Wang, Y., Seinfeld, J. H., and Zhang, R.: Unexpected Oligomerization of Small alpha-Dicarbonyls for Secondary Organic Aerosol and Brown Carbon Formation, Environmental Science & Technology, 55, 4430-4439, 10.1021/acs.est.0c08066, 2021.

460   Liggio, J., Li, S. M., and Mclaren, R.: Reactive uptake of glyoxal by particulate matter, Journal of Geophysical Research Atmospheres, 110, 2005a.

Liggio, J., Shao-Meng, L. I., and Mclaren, R.: Heterogeneous Reactions of Glyoxal on Particulate Matter: Identification of Acetals and Sulfate Esters, Environmental Science & Technology, 39, 1532-1541, 2005b.

Lim, Y. B., Tan, Y., and Turpin, B. J.: Chemical insights, explicit chemistry, and yields of secondary organic aerosol from OH
465   radical oxidation of methylglyoxal and glyoxal in the aqueous phase, Atmospheric Chemistry and Physics, 13, 8651-8667, 10.5194/acp-13-8651-2013, 2013.

Lim, Y. B., Kim, H., Kim, J. Y., and Turpin, B. J.: Photochemical organonitrate formation in wet aerosols, Atmospheric Chemistry and Physics, 16, 12631-12647, 10.5194/acp-16-12631-2016, 2016.

Lin, P., Laskin, J., Nizkorodov, S. A., and Laskin, A.: Revealing Brown Carbon Chromophores Produced in Reactions of
470   Methylglyoxal with Ammonium Sulfate, Environ Sci Technol, 49, 14257-14266, 10.1021/acs.est.5b03608, 2015.

Ling, Z., Xie, Q., Shao, M., Wang, Z., Wang, T., Guo, H., and Wang, X.: Formation and sink of glyoxal and methylglyoxal in a polluted subtropical environment: observation-based photochemical analysis and impact evaluation, Atmospheric Chemistry and Physics, 20, 11451-11467, 10.5194/acp-20-11451-2020, 2020.

Loeffler, K. W., Koehler, C. A., Paul, N. M., and Haan, D. D.: Oligomer formation in evaporating aqueous glyoxal and methyl
475   glyoxal solutions, Environmental Science & Technology, 40, 6318, 2006.

Lv, S., Gong, D., Ding, Y., Lin, Y., Wang, H., Ding, H., Wu, G., He, C., Zhou, L., Liu, S., Ristovski, Z., Chen, D., Shao, M.,

Zhang, Y., and Wang, B.: Elevated levels of glyoxal and methylglyoxal at a remote mountain site in southern China: Prompt in-situ formation combined with strong regional transport, Science of the Total Environment, 672, 869-882, 10.1016/j.scitotenv.2019.04.020, 2019.

480   Mitsuishi, K., Iwasaki, M., Takeuchi, M., Okochi, H., Kato, S., Ohira, S.-I., and Toda, K.: Diurnal Variations in Partitioning of Atmospheric Glyoxal and Methylglyoxal between Gas and Particles at the Ground Level and in the Free Troposphere, ACS Earth and Space Chemistry, 2, 915-924, 10.1021/acsearthspacechem.8b00037, 2018.

Odum, J. R., Hoffmann, T., Bowman, F., Collins, D., Flagan, R. C., and Seinfeld, J. H.: Gas/Particle Partitioning and Secondary Organic Aerosol Yields, Environmental Science & Technology, 30, 2580-2585, 1996.

485   Ortiz-Montalvo, D. L., Hakkinen, S. A., Schwier, A. N., Lim, Y. B., McNeill, V. F., and Turpin, B. J.: Ammonium addition (and aerosol pH) has a dramatic impact on the volatility and yield of glyoxal secondary organic aerosol, Environmental Science & Technology, 48, 255-262, 10.1021/es4035667, 2014.

Pankow and James, F.: An absorption model of the gas/aerosol partitioning involved in the formation of secondary organic aerosol, Atmospheric Environment, 28, 189-193, 1994.

490   Pankow, J. F.: An absorption model of GAS/Particle partitioning of organic compounds in the atmosphere, 1994.

Qian, X., Shen, H., and Chen, Z.: Characterizing summer and winter carbonyl compounds in Beijing atmosphere, Atmospheric Environment, 214, 10.1016/j.atmosenv.2019.116845, 2019.

Qiu, X., Wang, S., Ying, Q., Duan, L., Xing, J., Cao, J., Wu, D., Li, X., Chengzhi, X., Yan, X., Liu, C., and Hao, J.: Importance of Wintertime Anthropogenic Glyoxal and Methylglyoxal Emissions in Beijing and Implications for Secondary Organic

495   Aerosol Formation in Megacities, Environmental Science & Technology, 54, 11809-11817, 10.1021/acs.est.0c02822, 2020.

Rao, Z., Chen, Z., Liang, H., Huang, L., and Huang, D.: Carbonyl compounds over urban Beijing: Concentrations on haze and non-haze days and effects on radical chemistry, Atmospheric Environment, 124, 207-216, 10.1016/j.atmosenv.2015.06.050, 2016.

Sander, R.: Compilation of Henry's law constants (version 4.0) for water as solvent, Atmospheric Chemistry and Physics, 15,

500   4399-4981, 10.5194/acp-15-4399-2015, 2015.

Schwier, A. N., Sareen, N., Mitroo, D., Shapiro, E. L., and Mcneill, V. F.: Glyoxal-methylglyoxal cross-reactions in secondary organic aerosol formation, Environmental Science & Technology, 44, 6174-6182, 2010.

Shen, H., Chen, Z., Li, H., Qian, X., Qin, X., and Shi, W.: Gas-Particle Partitioning of Carbonyl Compounds in the Ambient Atmosphere, Environmental Science & Technology, 52, 10997-11006, 10.1021/acs.est.8b01882, 2018.

505   Shen, X., Wu, H., Zhao, Y., Huang, D., Huang, L., and Chen, Z.: Heterogeneous reactions of glyoxal on mineral particles: A new avenue for oligomers and organosulfate formation, Atmospheric Environment, 131, 133-140, 10.1016/j.atmosenv.2016.01.048, 2016.

Shi, Q., Zhang, W., Ji, Y., Wang, J., Qin, D., Chen, J., Gao, Y., Li, G., and An, T.: Enhanced uptake of glyoxal at the acidic nanoparticle interface: implications for secondary organic aerosol formation, Environmental Science: Nano, 7, 1126-1135,

510   10.1039/d0en00016g, 2020.

Tan, Y., Lim, Y. B., Altieri, K. E., Seitzinger, S. P., and Turpin, B. J.: Mechanisms leading to oligomers and SOA through aqueous photooxidation: insights from OH radical oxidation of acetic acid and methylglyoxal, Atmospheric Chemistry & Physics, 12, 801-813, 2012.

Teich, M., Pinxteren, D. V., Kecorius, S., Wang, Z., and Herrmann, H.: First Quantification of Imidazoles in Ambient Aerosol

515   Particles: Potential Photosensitizers, Brown Carbon Constituents, and Hazardous Components, Environmental Science & Technology, 50, 1166-1173, 2016.

Volkamer, R., San Martini, F., Molina, L. T., Salcedo, D., Jimenez, J. L., and Molina, M. J.: A missing sink for gas-phase glyoxal in Mexico City: Formation of secondary organic aerosol, Geophysical Research Letters, 34, 10.1029/2007gl030752,

2007.

520   Wang, H., Zhang, X., and Chen, Z.: Development of DNPH/HPLC method for the measurement of carbonyl compounds in
the aqueous phase: applications to laboratory simulation and field measurement, Environmental Chemistry, 6,
10.1071/en09057, 2009.

Williams, B. J., Goldstein, A. H., Kreisberg, N. M., and Hering, S. V.: In situ measurements of gas/particle-phase transitions
for atmospheric semivolatile organic compounds, Proceedings of the National Academy of Sciences, 107, 6676-6681,
525   10.1073/pnas.0911858107, 2010.

Xie, M., Hannigan, M. P., and Barsanti, K. C.: Gas/particle partitioning of 2-methyltetrols and levoglucosan at an urban site
in Denver, Environmental Science & Technology, 48, 2835-2842, 10.1021/es405356n, 2014.

Ying, Q., Li, J., and Kota, S. H.: Significant Contributions of Isoprene to Summertime Secondary Organic Aerosol in Eastern
United States, Environmental Science & Technology, 49, 7834-7842, 10.1021/acs.est.5b02514, 2015.

530   Zarzana, K. J., Selimovic, V., Koss, A. R., Sekimoto, K., Coggon, M. M., Yuan, B., Dubé, W. P., Yokelson, R. J., Warneke, C.,
de Gouw, J. A., Roberts, J. M., and Brown, S. S.: Primary emissions of glyoxal and methylglyoxal from laboratory
measurements of open biomass burning, Atmospheric Chemistry & Physics, 18, 15451-15470, 10.5194/acp-18-15451-2018,
2018.

Zarzana, K. J., Min, K. E., Washenfelder, R. A., Kaiser, J., Krawiec-Thayer, M., Peischl, J., Neuman, J. A., Nowak, J. B.,
535   Wagner, N. L., Dube, W. P., St Clair, J. M., Wolfe, G. M., Hanisco, T. F., Keutsch, F. N., Ryerson, T. B., and Brown, S. S.:
Emissions of Glyoxal and Other Carbonyl Compounds from Agricultural Biomass Burning Plumes Sampled by Aircraft,
Environmental Science & Technology, 51, 11761-11770, 10.1021/acs.est.7b03517, 2017.

Zhao, J., Levitt, N. P., Zhang, R., and Chen, J.: Heterogeneous reactions of methylglyoxal in acidic media: implications for
secondary organic aerosol formation, Environmental Science & Technology, 40, 7682-7687, 2006.

540   Zhu, Y., Yang, L., Chen, J., Kawamura, K., Sato, M., Tilgner, A., van Pinxteren, D., Chen, Y., Xue, L., Wang, X., Simpson, I.
J., Herrmann, H., Blake, D. R., and Wang, W.: Molecular distributions of dicarboxylic acids, oxocarboxylic acids and α-
dicarbonyls in PM2.5 collected at the top of Mt. Tai, North China, during the wheat burning season of 2014, Atmospheric
Chemistry and Physics, 18, 10741-10758, 10.5194/acp-18-10741-2018, 2018.
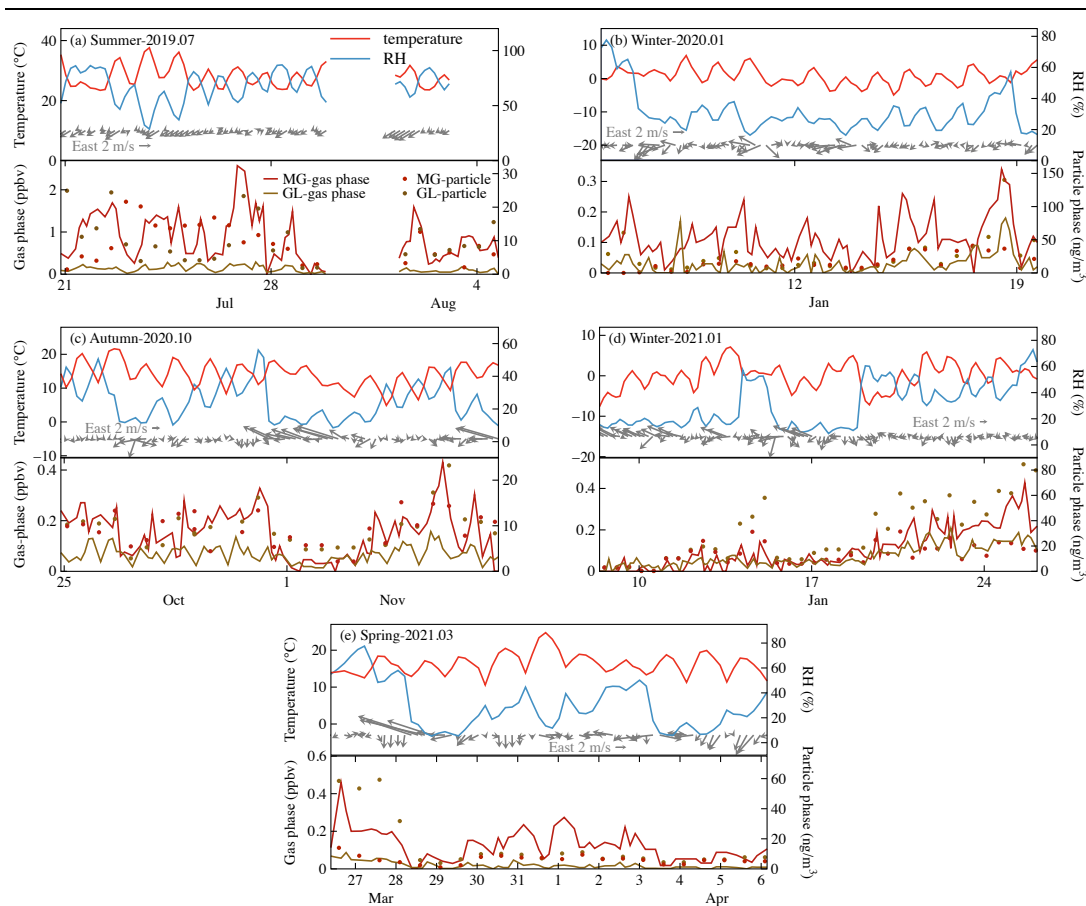
545

Figure 1: Time series of meteorological parameters and gas- and particle-phase glyoxal and methylglyoxal observed in different seasons: (a) summer, 2019.07.20-2019.08.04; (b) winter, 2020.01.05-2020.01.19; (c) autumn, 2020.10.24-2020.11.07; (d) winter, 2021.01.08-2021.01.26; (e) spring, 2021.03.26-2021.04.06. The lines and solid circles indicate the gaseous carbonyls (ppbv) and particulate carbonyls (ng/m³), respectively.
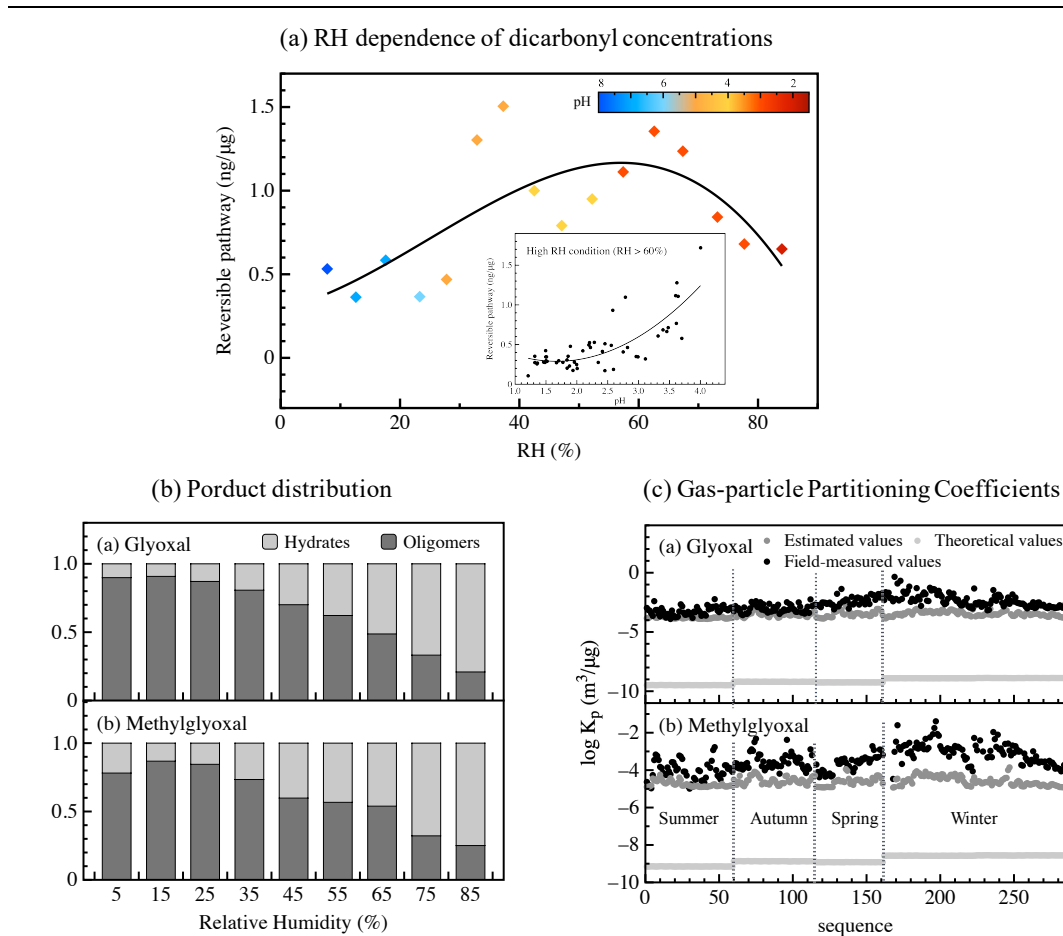
Figure 2: Gas-particle partitioning of dicarbonyls via reversible pathways. (a) The RH dependence of total particulate dicarbonyl concentrations and their pH dependence under high RH conditions. (b) The product distribution for (i) glyoxal and (ii) methylglyoxal under different RH conditions. (c) The gas-particle partitioning coefficients for (i) glyoxal and (ii) methylglyoxal. The black, dark gray, and light gray circles refer to field-measured values, estimated values by the proposed mechanism, and theoretical values calculated by Pankow's absorptive model, respectively.
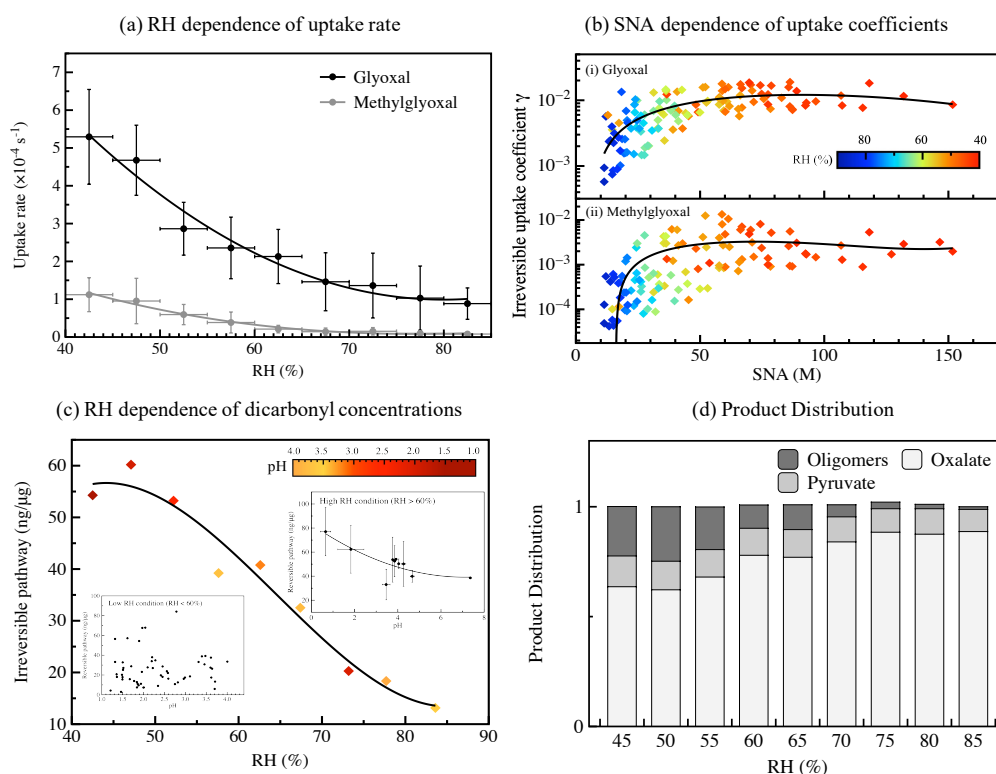
Figure 3: Gas-particle partitioning of dicarbonyls via irreversible pathways. (a) The RH dependence of irreversible uptake rate for glyoxal and methylglyoxal. (b) The SNA dependence of uptake coefficients for (i) galyoxal and (ii) methylglyxoal. (c) The correlation between oxalate concentrations measured by ion chromatography (gray lines) and those calculated by modeling coupled with the full kinetic of glyoxal/methylglyoxal + OH (black lines). (d) The corresponding modeled product distribution and O/C (on the right-hand y-axis) in wet aerosols under different RH conditions.
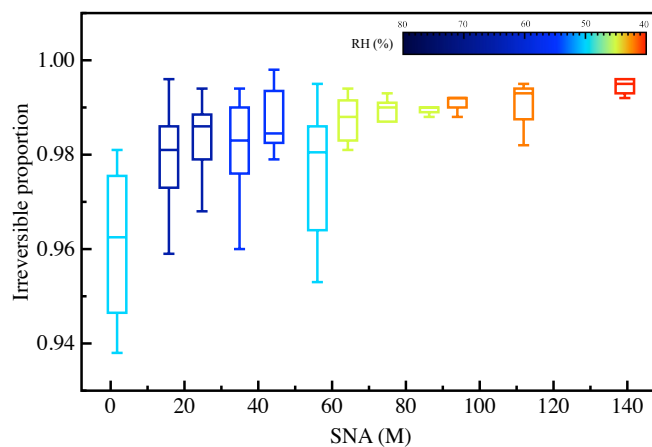
Figure 4: Correlation between the proportion of the irreversible pathway in gas-particle partitioning process for dicarbonyls

565   and aqueous sulfate, nitrate, and ammonia (SNA) concentration in ambient aerosols under different relative humidity

conditions.

Table 1: Statistical data for the α-dicarbonyls in gas and particle phase in different seasons.

Season	Gas phase (ppbv)			Particle phase (ng m^{-3})		
	GL	MG	GL:MG	GL	MG	GL:MG
summer	0.13 ± 0.07	0.87 ± 0.54	0.15	10.18 ± 6.63	9.50 ± 5.62	1.07
spring	0.02 ± 0.02	0.12 ± 0.08	0.17	15.24 ± 17.50	6.07 ± 2.79	2.51
autumn	0.07 ± 0.03	0.15 ± 0.09	0.47	9.33 ± 4.24	9.15 ± 3.62	1.02
winter	0.06 ± 0.05	0.11 ± 0.09	0.54	28.77 ± 25.33	14.61 ± 10.15	1.97

570   Table 2: Comparison of the field-measured partitioning coefficient K^f values for the dicarbonyls and their corresponding theoretical K^t values in different seasons.

Coefficients	Dicarbonyl	Season	K^f		K^t	K^f/K^t
			Average	Range		
Gas-particle partitioning coefficients ($m^3 \cdot \mu g^{-1}$)	glyoxal	summer	8.11×10^{-4}	$(1.25-58.6) \times 10^{-4}$	3.27×10^{-10}	2.48×10^{6}
		autumn	2.14×10^{-3}	$(2.61-224) \times 10^{-4}$	6.27×10^{-10}	3.41×10^{6}
		spring	1.43×10^{-2}	$(0.08-14.6) \times 10^{-2}$	5.59×10^{-10}	3.55×10^{7}
		winter	1.30×10^{-2}	$(0.067-44.2) \times 10^{-2}$	1.27×10^{-9}	1.02×10^{7}
	methylglyoxal	summer	1.49×10^{-4}	$(0.833-169) \times 10^{-5}$	7.10×10^{-10}	2.10×10^{5}
		autumn	9.55×10^{-4}	$(0.65-86.9) \times 10^{-4}$	1.35×10^{-9}	7.07×10^{5}
		spring	1.06×10^{-3}	$(0.42-108) \times 10^{-4}$	1.21×10^{-9}	8.77×10^{5}
		winter	2.60×10^{-3}	$(0.34-410) \times 10^{-4}$	2.72×10^{-9}	9.93×10^{5}
Henry's law coefficients ($M \cdot atm^{-1}$)	glyoxal	summer	1.96×10^{8}	$(1.71-167) \times 10^{7}$	3.29×10^{5}	6.11×10^{2}
		autumn	5.08×10^{8}	$(1.88-10.2) \times 10^{8}$	1.14×10^{6}	3.63×10^{3}
		spring	2.53×10^{9}	$(1.23-139) \times 10^{8}$	9.03×10^{5}	1.92×10^{4}
		winter	1.04×10^{9}	$(1.37-55.4) \times 10^{8}$	4.15×10^{6}	2.55×10^{3}
	methylglyoxal	summer	4.92×10^{7}	$(1.70-363) \times 10^{6}$	2.73×10^{3}	1.88×10^{4}
		autumn	8.52×10^{7}	$(3.66-15.7) \times 10^{7}$	9.50×10^{3}	2.00×10^{5}
		spring	1.33×10^{8}	$(5.22-456) \times 10^{6}$	7.49×10^{3}	1.36×10^{5}
		winter	2.63×10^{8}	$(1.03-175) \times 10^{7}$	3.44×10^{4}	9.01×10^{4}

Table 3: Summary of calculated uptake coefficients γ and effective uptake rate coefficient $k_{eff, uptake}$ in different seasons for glyoxal and methylglyoxal.

Dicarbonyl	Season	T (K)	RH (%)	γ (×10^{-3})			$k_{eff, uptake}$ (s^{-1})
				Average	Min	Max	(×10^{-4})
GL	Summer	301.1	67.7	4.15	0.12	7.30	1.61
	Autumn	287.2	45.4	8.62	0.29	12.9	4.83
	Spring	289.4	54.0	11.7	1.24	14.9	6.85
	Winter	273.5	54.0	10.6	0.56	14.4	3.59
	[a] **General**	**287.8**	**59.0**	**8.0**	**0.46**	**11.4**	**3.38**
MG	Summer	301.1	67.7	1.01	0.02	2.09	0.25
	Autumn	287.2	45.4	1.83	0.04	3.94	0.92
	Spring	289.4	54.0	2.36	0.06	4.34	0.69
	Winter	273.5	54.0	3.45	0.11	5.83	0.77
	[a] **General**	**287.8**	**59.0**	**2.0**	**0.05**	**3.8**	**0.55**

575   [a] General is the average value of all the samples observed in the five field observations.

Table 4: Calculated relative importance of reversible and irreversible pathways in the gas-particle partitioning processes and their contribution to the particle matter.

Season	Glyoxal		Methylglyoxal		Contribution to
	[a] $[X]_{P, rever}$	[b] $[X]_{P, irrever}$	[a] $[X]_{P, rever}$	[b] $[X]_{P, irrever}$	particulate matters
Summer	0.17 (1.2%)	18.87 (98.8%)	0.25 (5.5%)	20.55 (94.5%)	3.98%
Autumn	0.14 (0.7%)	23.91(99.3%)	0.12 (0.8%)	17.02 (99.2%)	4.12%
Spring	0.26 (1.9%)	15.94 (98.1%)	0.09 (1.5%)	14.16 (98.5%)	3.05%
Winter	0.89 (7.1%)	34.70 (92.9%)	0.38 (7.2%)	12.59 (92.8%)	4.86%
[c] **General**	**0.43 (3.3%)**	**24.26 (96.7%)**	**0.25 (5.0%)**	**16.53 (95.0%)**	**4.15%**

[a] $[X]_{P, rever}$ is the concentration of particle-phase carbonyl via reversible pathway (ng·μg^{-1}) and its proportion (%).

580 [b] $[X]_{P, irrever}$ is the concentration of particle-phase carbonyl via irreversible pathway (ng·μg^{-1}) and its proportion (%).

[c] General is the average value of all the samples observed in the five field observations.